

Received March 26, 2017, accepted April 15, 2017, date of publication April 25, 2017, date of current version June 7, 2017.

Digital Object Identifier 10.1109/ACCESS.2017.2697975

# A Robust Active Contour Segmentation Based on Fractional-Order Differentiation and Fuzzy Energy

HONGLI LV<sup>1</sup>, ZIYU WANG<sup>2</sup>, SHUJUN FU<sup>1</sup>, CAIMING ZHANG<sup>3</sup>, LIN ZHAI<sup>1</sup>, AND XUYA LIU<sup>1</sup>

<sup>1</sup>School of Mathematics, Shandong University, Jinan 250100, China

<sup>2</sup>Department of Radiology, Yidu Central Hospital of Weifang, Qingzhou 262500, China

<sup>3</sup>School of Computer Science and Technology, Shandong University, Jinan 250101, China

Corresponding author: Shujun Fu (shujunfu@163.com)

This work was supported in part by the National Natural Science Foundation of China under Grant 61272239, Grant 61070094, and Grant 61671276, in part by the Science and Technology Development Project of Shandong Province of China under Grant 2014GGX101024, and in part by the Fundamental Research Funds of Shandong University under Grant 2014JC012.

**ABSTRACT** Vascular diseases cause a wide range of severe health problems. Vessel images are often corrupted by intensity inhomogeneity and blurry boundary, which makes it difficult to segment vessel image to identify vascular lesions. Integrating the fuzzy decision and a special local energy functional, in this paper, a robust active contour model is proposed to segment preprocessed vessel images. First, as for the blurry boundary problem, unlike the traditional method, a fractional-order differential method is used to enhance the original image for accurate segmentation utilizing fully high-frequency marginal features. Then, to deal with intensity inhomogeneity, a novel energy functional is formulated by considering the local fuzzy statistical information of boundaries. At the same time, a double-well potential function is designed to automatically limit the values of the membership function in the range  $[0, 1]$  during the curve evolution. Finally, Experiments on synthetic and real images are carried out, showing the accuracy of the proposed model and the robustness to the initial contour when working on vascular images.

**INDEX TERMS** Active contour, vascular segmentation, fuzzy energy, double-well potential function, fractional-order differentiation.

## I. INTRODUCTION

Vascular disease is a pathological state of large and medium muscular arteries and is triggered by endothelial cell dysfunction [1]. Disorders in this vast network of blood vessels can cause a range of health problems which can be severe or prove fatal. For example, cardiovascular disease causes more than 17 million deaths in the world each year [2]. In addition, the evaluation of vascular abnormalities (such as stenoses and plaques) is heavily dependent on the quality of vessel segmentation, which also affects the results of the following high level tasks, such as computer-aided diagnosis, surgery planning and treatment. Therefore, vessel segmentation is one of demanding applications that has received a considerable attention [3], [4]. Until now, a large number of methodologies have been proposed for vessel segmentation, such as tubular structure [5], [6], pattern recognition [7], [8] and centerline based approaches [9], [10]. Due to instrumental limitations, vessel images are often corrupted by intensity inhomogeneity, which makes the segmentation of vascular images to be a challenging problem in medical image domain.

In the literature, active contour models (ACMs) [11], [12] and fuzzy clustering [13], [14] have gained more attention as their good experimental performance and sound theoretical foundation. Among the fuzzy clustering methods, Fuzzy c-means (FCM) [15] algorithm is one of the most widely used methods in image segmentation because of its well performance. Although FCM can retain more information from original image than hard clustering method, it fails to segment images with intensity inhomogeneity. On the other hand, a great deal of attention has been paid to ACMs thanks to their impressive achievements in terms of accuracy. The basic idea of ACMs consists in implicitly representing a curve as the zero level set of a higher dimensional function, called level set function (LSF) [16]. By minimizing the defined energy functional, a partial differential equation can be obtained to drive the evolution of the curve.

Generally speaking, the existing ACMs can be roughly classified into two categories: edge-based models [17], [18] and region-based models [19]–[23]. Edge-based ACMs utilize image gradient information to guide the evolution curve

toward the boundaries of the interested objects. Consequently, they have difficulty in detecting weak boundary and are sensitivity to the noise. Region-based ACMs use a certain region-based image information to guide the curve evolution toward the desired boundaries. Comparing with edge-based ACMs, region-based ACMs generally offer better performance in the case of weak object boundaries. One of the most popular region-based ACMs is the Chan-Vese (CV) model [19]. More recently many fuzzy logic based ACMs are proposed to enhance the robustness of the model [24]–[28]. For example, S. Krinidis and V. Chatzis [24] proposed a fuzzy energy-based active contour model (FEBAC), Wu *et al.* [27] proposed another fuzzy active contour model with kernel metric (KFAC). Just like the CV model, they have difficulty in dealing with intensity inhomogeneous images, since they rely on global information of images. In case of intensity inhomogeneity, global information may be far different from the actual data of image. In fact, intensity inhomogeneity images are frequently observed in vessel images [29]. In [28] a selective level set segmentation (SLSS) method, using fuzzy region competition, is proposed to cope with this problem. Unfortunately, the SLSS model still suffers from some drawbacks in face of inhomogeneity. Many studies have shown that incorporating local image information into the energy functional is an effective way to tackle intensity inhomogeneity. The local binary fitting model (LBF) [20], [21] is a well-known local information based active contour model, which gets desirable segmentation results of images with intensity inhomogeneity. The main drawback of LBF model is highly dependent on the initial contour.

Vessel images often exhibit low contrast, which makes it difficult to segment vessel. A large number of contrast enhancement techniques have been proposed to overcome this problem [30]. Recently, methods based on fractional differentiation [31], [32] are proposed to deal with the problem of low contrast and give better performance than traditional ones. Fractional order differentiation is a generalization of the ordinary differentiation and can provide the best description for many natural phenomena. Due to more precisely derivatives of arbitrary order, fractional order differential methods can retain high-frequency marginal features in the areas of gray-level dramatic changes and preserve low-frequency features in smooth areas [31]–[35].

In the present work, a robust fuzzy active contour model is proposed to segment vessel images. Because the fractional-order differential methods preserve not only low-frequency but also high-frequency features of images [31]–[35], we construct a fractional-order mask to enhance vessel image. Then, the enhanced image is used to define the local statistical information and to guide the curve evolution. As mentioned above, incorporating local image information into the energy functional is an effective way to tackle intensity inhomogeneity and soft clustering method can retain more information from original image. We propose a local fuzzy energy functional integrating the advantage of local-based ACMs and fuzzy energy-based ACMs. By taking the local

fuzzy intensity information into account, the proposed model can better deal with intensity inhomogeneity. In addition, the Gaussian filtering method is used to regularize the pseudo level set function, which can keep the level set function smoothing in the evolution of curve. Noting that the membership function  $u$  may break the constraint ( $0 \leq u \leq 1$ ) during the curve evolution, we define a new embedded penalty function to limit the pseudo level set function in the range  $[0, 1]$ , which makes the proposed model more robust. The advantage of the proposed model compared with the FEBAC model and the classic CV model is that it can segment images with intensity inhomogeneity. Compared with the well-known LBF model, the proposed model is more robustness to the initial contour.

In summary, the main contributions of the paper are as follows. (1) We use the filtered image resulting from fractional order differentiation as a guide image to accurately estimate the local fuzzy information. The increased quality of this guide image improves the performance of the proposed model. (2) We combine the idea of the local-based ACMs and the fuzzy-based ACMs into the energy functional which can exploit the benefits of both methods. (3) Based on the observation of the membership function, we propose a new embedded penalty function to limit it in the range  $[0, 1]$ , which makes the proposed model more robust.

The remainder of this paper is organized as follows. Section 2 gives a brief review on related works and indicates their limitations. We describe the proposed active contour model for vessel segmentation in details in Section 3. Section 4 presents the experimental results and the comparisons on real and synthetic images. Finally, conclusions are drawn in Section 5.

## II. BACKGROUND

Active contour model is computer-generated curves that move within images to find object boundaries. It is popular in computer vision, and is greatly used in applications like object tracking, shape recognition, edge detection and segmentation. The basic idea of the related works and the proposed method is to implicitly represent an evolving curve as the zero level set of a higher dimension level set function, and an evolving curve is driven by a partial differential equation obtained by minimizing a predefined energy functional. In this section, we will give a brief review on related works for image segmentation and also indicate their limitations.

### A. CV MODEL

By simplifying the Mumford-Shah model [22], Chan and Vese [19] proposed a region-based active contour model. They defined the following energy functional

$$E^{CV}(\phi, c_1, c_2) = \lambda_1 \int_{\Omega} |I(x) - c_1|^2 H_{\varepsilon}(\phi(x)) dx + \lambda_2 \int_{\Omega} |I(x) - c_2|^2 (1 - H_{\varepsilon}(\phi(x))) dx \quad (1)$$

where  $\lambda_1 > 0$ ,  $\lambda_2 > 0$ , are fixed parameters.  $I(x)$  is the intensity at a point  $x$ .  $c_1$  and  $c_2$  are the average intensities

inside and outside the contour  $C = \{x \in \Omega : \phi(x) = 0\}$ . Normally, the level set function  $\phi$  is initialized as the signed distance function

$$\phi(x) = \begin{cases} +distance(x, C), & x \in interior\ of\ C \\ -distance(x, C), & x \in exterior\ of\ C \end{cases} \quad (2)$$

The modified Heaviside function  $H_\epsilon(\phi)$  is defined by

$$H_\epsilon(z) = \frac{1}{2} \left( 1 + \frac{2}{\pi} \arctan \left( \frac{z}{\epsilon} \right) \right), \quad z \in \mathbb{R} \quad (3)$$

The assumption of the CV model is that image intensity is constant in foreground and background. Although it is robust against noise and less sensitive to initial contour, it does not work well on images intensity inhomogeneity.

### B. FEBAC MODEL

The FEBAC model [24] is a fuzzy energy-based active contour model, which divides the image into foreground and background. Different from the CV model [19] which uses the sign distance function [36] as the initial level set function, the curve  $C$  is implicitly represented by the pseudo zero level set function, such that

$$\begin{cases} C = \{x \in \Omega : u(x) = 0.5\} \\ inside(C) = \{x \in \Omega : u(x) > 0.5\} \\ outside(C) = \{x \in \Omega : u(x) < 0.5\} \end{cases} \quad (4)$$

and the fuzzy energy functional is defined as follows

$$E^{FEBAC}(u, c_1, c_2) = \lambda_1 \int_{\Omega} [u(x)]^m |I(x) - c_1|^2 dx + \lambda_2 \int_{\Omega} [1 - u(x)]^m |I(x) - c_2|^2 dx \quad (5)$$

where  $\lambda_1 > 0, \lambda_2 > 0$  are fixed parameters.  $u(x)$  is the degree of the membership of pixel  $x$  belong to  $c_1$ , and  $1 - u(x)$  is the degree of the membership of pixel  $x$  belong to  $c_2$ .  $m$  is a weighting exponent on each fuzzy membership, which is usually set to 2. Keeping  $u$  fixed and minimizing the energy functional (5) with respect to  $c_1$  and  $c_2$ , we obtain the updating equations of  $c_1, c_2$  as follows

$$c_1 = \frac{\int_{\Omega} [u(x)]^m I(x) dx}{\int_{\Omega} [u(x)]^m dx}, \quad c_2 = \frac{\int_{\Omega} [1 - u(x)]^m I(x) dx}{\int_{\Omega} [1 - u(x)]^m dx} \quad (6)$$

It can be observed that the constant  $c_1, c_2$  are the average intensity inside and outside the contour  $C$ . Like the CV model, the FEBAC model is proposed with assumption that foreground and background are homogeneous. Consequently, the FEBAC model still fails to segment images with intensity inhomogeneity. The KFAC model, proposed in [27], is similar to the FEBAC model. Although the KFAC model is more robust to images in the presence of noise than the CV model and the FEBAC model, it also fails to deal with intensity inhomogeneity because only global information is used.

### C. LBF MODEL

To solve the drawback of the global information based models, which have undesirable performance on images with intensity inhomogeneity, Li et al. proposed the LBF model [20], [21]. The local statistical information is obtained by introducing a kernel function. They defined the energy functional as follows

$$E^{LBF}(\phi, f_1, f_2) = \lambda_1 \int_{\Omega} \int_{\Omega} K_{\sigma}(x - y) |I(y) - f_1(x)|^2 H_{\epsilon}(\phi(y)) dy dx + \lambda_2 \int_{\Omega} \int_{\Omega} K_{\sigma}(x - y) |I(y) - f_2(x)|^2 (1 - H_{\epsilon}(\phi(y))) dy dx \quad (7)$$

where  $K_{\sigma}$  is the Gaussian kernel function with standard deviation  $\sigma, \lambda_1 > 0, \lambda_2 > 0$  are fixed parameters. Keeping level set function  $\phi$  fixed and minimizing the energy functional (7) with regard to local center  $f_1$  and  $f_2$ , we can obtain the following equation

$$f_1(x) = \frac{\int_{\Omega} K_{\sigma}(x - y) I(y) H_{\epsilon}(\phi(y)) dy}{\int_{\Omega} K_{\sigma}(x - y) H_{\epsilon}(\phi(y)) dy} \quad f_2(x) = \frac{\int_{\Omega} K_{\sigma}(x - y) I(y) (1 - H_{\epsilon}(\phi(y))) dy}{\int_{\Omega} K_{\sigma}(x - y) (1 - H_{\epsilon}(\phi(y))) dy} \quad (8)$$

Though the LBF model can effectively segment inhomogeneous images, it is sensitive to initial contour.

### III. THE PROPOSED MODEL

In order to overcome the drawbacks of the active contour models discussed in section 2, in this section, we present a novel fuzzy energy based active contour model and describes it in details. We firstly introduce the fractional order differential method used to enhance image. Then, we formulate a new local-based energy functional and define a new penalty function.

#### A. FRACTIONAL-ORDER DIFFERENTIATION

The fractional order differentiation is a generalization of the ordinary differentiation. The definition of fractional order differentiation is studied by many researchers from different views and more than one exist in the literature. In this paper, we use Grünwald-Letnikov (GL) definition [31], which can be expressed as

$${}_{t_0}D_t^{\nu} s(t) = \lim_{h \rightarrow 0} \frac{1}{h^{\nu}} \sum_{j=0}^{[(t-t_0)/h]} (-1)^j \binom{\nu}{j} s(t - jh) \quad (9)$$

where  $\binom{\nu}{j} = \frac{\Gamma(\nu+1)}{\Gamma(j+1)\Gamma(\nu-j+1)}, 0 < \nu \leq 1, \Gamma$  is the Gamma function. The explicit numerical approximation can be expressed as

$${}_{t_0}D_t^{\nu} s(t) \approx \frac{1}{h^{\nu}} \sum_{j=0}^{[(t-t_0)/h]} w_j^{(\nu)} s(t - jh) \quad (10)$$

$w_n^v$	0	...	0	$w_n^v$	0	...	0	$w_n^v$
0	$\ddots$	$\ddots$	$\vdots$	$\vdots$	$\vdots$	$\ddots$	$\ddots$	0
$\vdots$	$\ddots$	$w_3^v$	0	$w_3^v$	0	$w_3^v$	$\ddots$	$\vdots$
0	...	0	$w_2^v$	$w_2^v$	$w_2^v$	0	...	0
$w_n^v$	...	$w_3^v$	$w_2^v$	$8w_1^v$	$w_2^v$	$w_3^v$	...	$w_n^v$
0	...	0	$w_2^v$	$w_2^v$	$w_2^v$	0	...	0
$\vdots$	$\ddots$	$w_3^v$	0	$w_3^v$	0	$w_3^v$	$\ddots$	$\vdots$
0	$\ddots$	$\ddots$	$\vdots$	$\vdots$	$\vdots$	$\ddots$	$\ddots$	0
$w_n^v$	0	...	0	$w_n^v$	0	...	0	$w_n^v$

FIGURE 1. Fractional order enhancement mask  $W$ .

where  $w_j^v = (-1)^j \binom{v}{j}$ . Setting  $h = 1$  and  $n = [t - t_0]$ , the  $v$  order fractional differential expression of two-dimensional signal  $s(p, q)$  can be expressed as

$$\begin{aligned} \frac{\partial^v s(p, q)}{\partial p^v} \approx & s(p, q) + (-v)s(p-1, q) + \frac{(-v)(-v+1)}{2}s(p-2, q) \\ & + \frac{(-v)(-v+1)(-v+2)}{6}s(p-3, q) + \dots \\ & + \frac{\Gamma(-v+1)}{n!\Gamma(-v+n+1)}s(p-n, q) \end{aligned} \quad (11)$$

$$\begin{aligned} \frac{\partial^v s(p, q)}{\partial q^v} \approx & s(p, q) + (-v)s(p, q-1) + \frac{(-v)(-v+1)}{2}s(p, q-2) \\ & + \frac{(-v)(-v+1)(-v+2)}{6}s(p, q-3) + \dots \\ & + \frac{\Gamma(-v+1)}{n!\Gamma(-v+n+1)}s(p, q-n) \end{aligned} \quad (12)$$

We can find that the corresponding coefficients of the  $v$  order fractional partial differential on negative  $p$  and  $q$  coordinate is same. These coefficients can be got from (11) and (12)

$$w_0^v = 1, w_1^v = -v, \dots, w_n^v = \frac{\Gamma(-v+1)}{n!\Gamma(-v+n+1)} \quad (13)$$

The fractional enhancement mask  $W$  can be constructed as it shown in Figure 1. Obviously, the defined mask is rotation invariant, and the filtered value of the pixel  $I(p, q)$  can be calculated using

$$D^v I(p, q) = \sum_{i=-\frac{n-1}{2}}^{\frac{n-1}{2}} \sum_{j=-\frac{n-1}{2}}^{\frac{n-1}{2}} W(i, j)I(p+i, q+j) \quad (14)$$

where  $W$  is the mask shown in Figure 1 and  $n$  (and odd integer) is the size of the mask. From (13), we can find that these coefficients are nonzero and the summation is also nonzero. As far as possible to ensure the intensity of  $I(p, q)$  is within  $[0, 255]$ , the filtered image is divided by the summation of these nonzero coefficients. Therefore, (14) can be rewritten

as

$$\begin{aligned} D^v I(p, q) &= \left( \sum_{i=-\frac{n-1}{2}}^{\frac{n-1}{2}} \sum_{j=-\frac{n-1}{2}}^{\frac{n-1}{2}} W(i, j)I(p+i, q+j) \right) / \left( 8 \sum_{i=0}^n w_i^v \right) \end{aligned} \quad (15)$$

It is not difficult to find that the bigger the mask size is, the higher degree of accuracy will be obtained, but the computation time will be consuming. In this paper, we select the size of  $n = 5$ . Selecting an appropriate parameter  $v$  is also a difficult task. There is no doubt that one value cannot fit all images. Fortunately,  $v = 0.2$  is appropriate for all experiments in this paper.

### B. ENERGY FORMULATION

Recall that local image information is the key to segment images with intensity inhomogeneity. Like the LBF model [20], [21], we define the following local fuzzy energy functional by using a Gaussian kernel.

$$\begin{aligned} E^{Local}(u, f_1, f_2) &= \lambda_1 \int_{\Omega} \int_{\Omega} K_{\sigma}(x-y) |D^v I(y) - f_1(x)|^2 [u(y)]^m dy dx \\ &+ \lambda_2 \int_{\Omega} \int_{\Omega} K_{\sigma}(x-y) |D^v I(y) - f_2(x)|^2 [1-u(y)]^m dy dx \end{aligned} \quad (16)$$

where  $\lambda_1 > 0, \lambda_2 > 0$  are fixed parameters.  $K_{\sigma}$  is a Gaussian kernel with standard deviation  $\sigma$ . In this paper,  $\sigma$  is set to 5.  $f_1(x)$  and  $f_2(x)$  are two smooth functions that fit the local statistical prototypes of the image  $D^v I$  inside and outside the contour  $C$ .  $u$  and  $1-u$  are the degree of the membership of pixel  $x$  belong to  $f_1(x)$  and  $f_2(x)$ , respectively.  $m$  is a weighting exponent on each fuzzy membership. For the fixed membership function  $u$ , by minimizing the fuzzy energy functional (16) with respect to the function  $f_1(x)$  and  $f_2(x)$ , we get the updating equations of  $f_1(x)$  and  $f_2(x)$  as follows

$$\begin{aligned} f_1(x) &= \frac{\int_{\Omega} K_{\sigma}(x-y) D^v I(y) [u(y)]^m dy}{\int_{\Omega} K_{\sigma}(x-y) [u(y)]^m dy} \\ f_2(x) &= \frac{\int_{\Omega} K_{\sigma}(x-y) D^v I(y) [1-u(y)]^m dy}{\int_{\Omega} K_{\sigma}(x-y) [1-u(y)]^m dy} \end{aligned} \quad (17)$$

$f_1(x)$  and  $f_2(x)$  given by (17) are two local fuzzy clustering center functions, which compute the local intensity means inside and outside the contour  $C$  defined in (4) in a neighborhood of  $x$ . Local information based model, which can get well performance on segmenting images with intensity inhomogeneity, are sensitive to the initial contour. But our model is based on fuzzy clustering method, which can deal with this problem, as shown in section 4.

Note that the fuzzy membership function  $u$  may break the constraint ( $0 \leq u \leq 1$ ) during the curve evolution, in [27] they set  $u = 0$ , if  $u < 0$  and  $u = 1$ , if  $u > 1$  after updating  $u$ . However, this crude approach will reduce the stability of the

level set evolution. In this paper, we propose an embedded penalty function to automatically limit  $u$  in the range  $[0, 1]$ , which makes the proposed model more robust. The penalty function is defined by

$$R(u) = \int_{\Omega} p(u(x))dx \quad (18)$$

with

$$p(s) = \frac{1}{4}(s(s - 1))^2 \quad (19)$$

The function (19) is a double-well potential function, which has two minimum points  $s = 0$  and  $s = 1$ . When minimizing the penalty energy term (18), it can be observed that values less than zero are driven toward 0 and values greater than 1 are driven toward 1. Thus, the values of  $u$  can be limit in the range  $[0, 1]$ .

The whole fuzzy energy functional is expressed by

$$E(u, f_1, f_2) = \alpha E^{Local}(u, f_1, f_2) + \beta R(u) \quad (20)$$

where  $\alpha > 0, \beta > 0$  are fixed parameters. Keeping  $f_i$  ( $i = 1, 2$ ) fixed, we minimize the energy functional (20) with respect to  $u$ , we obtain the following formulation

$$\frac{\partial u}{\partial t} = \alpha[-m(u(x))^{m-1}\lambda_1 e_1(x) + m(1 - u(x))^{m-1}\lambda_2 e_2(x)] - \beta[\frac{1}{2}u(x)(2u(x) - 1)(u(x) - 1)] \quad (21)$$

where  $e_i(x)$  ( $i = 1, 2$ ) are the functions

$$e_i(x) = \int_{\Omega} K_{\sigma}(y - x)|D^{\nu}I(x) - f_i(y)|^2 dx, \quad i = 1, 2 \quad (22)$$

here,  $f_1$  and  $f_2$  are given by (17).

### C. ALGORITHM

Before the evolution of curve, the normalization of the input image is applied for a stable updating of  $u$ , and the Gaussian filtering method [23] is used to smooth the pseudo level set function. The filtering process can be expressed as

$$u^{k+1} = K_{\xi} u^k \quad (23)$$

where  $\xi$  is the standard deviation,  $k$  is the number of iterations. In this paper, we set  $\xi = 0.5$  for all experiments. (21) is solved by a finite difference scheme. In the image domain, the spacial partial derivative  $\partial u/\partial x$  and  $\partial u/\partial y$  are approximated by the central difference with fixed space steps  $\Delta x = \Delta y = 1$ . The temporal partial derivative  $\partial u/\partial t$  is approximated by the forward difference with time step  $\Delta t = 1$ . Therefore, (21) can be discretized as a finite equation defined as follows

$$\frac{u_{i,j}^{k+1} - u_{i,j}^k}{\Delta t} = A(u_{i,j}^k). \quad (24)$$

where  $A(u_{i,j}^k)$  is the approximation of the right hand side in (21). The steps of the proposed model are as follows

1. *Normalize the original image.*

2. *Initialize the pseudo level set function, set  $u > 0.5$  for one part and  $u < 0.5$  for the other part. Initialize  $f_i$  ( $i = 1, 2$ ).*

3. *Update  $u_{i,j}^{k+1} = u_{i,j}^k + \Delta t \cdot A(u_{i,j}^k)$ .*

4. *Update  $f_i$  ( $i = 1, 2$ ) by (17).*

5. *Smooth the level set function  $u$  by (23).*

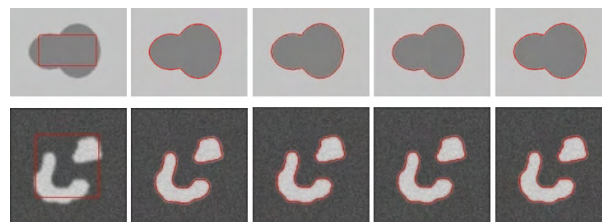
6. *Check whether the evolution is stationary. If not, return to step 3.*

## IV. EXPERIMENTAL RESULTS

This section shows the experimental results of the proposed model. To validate the effectiveness of the proposed model, we compare the proposed model with two classical active contour models and a fuzzy energy based model: global energy based model (CV model [19]), local energy based model (LBF model [20]), fuzzy energy based model (FEBAC model [24], KFAC [27], SLSS [28]). All the experiments are carried out by Matlab (R2014b) in the PC with Dual 3.2 GHz processor. The parameters are set as follows:  $m = 2, \lambda_1 = \lambda_2 = 1, \alpha = \beta = 1$ . According to the segmentation results,  $\nu = 0.2$  is appropriate for all experiments. The parameters of the compared methods are set according to the original papers.

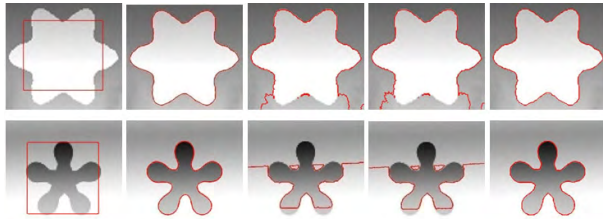
### A. APPLICATION ON SYNTHETIC IMAGES

Figure 2 shows the results of two homogeneous images. Figure 3 shows the results of images with intensity inhomogeneity. The first column shows the original images with the same initial contour. The second column to the last column show the segmentation results of our model, CV model, FEBAC model and LBF model, respectively. From Figure 2, it can be observed that all methods work well on two homogeneous images. Two images showed in Figure 3 are corrupted by intensity inhomogeneity. It can be seen that our model and LBF model obtain satisfactory segmentation results. However, CV model and FEBAC model fail to segment them due to only using the global mean of intensities. Using local image information ensures our model and the LBF model to effectively extract the object boundaries.



**FIGURE 2.** Segmentation results on homogeneous images. First column: original images with initial contour. Second column to fifth column: segmentation results of our model, CV model, FEBAC model and LBF model, respectively.

Figure 4 shows the comparisons with FEBAC model and KFAC model. The top row shows that our model and KFAC model work well on images in the presence of noise. Incorporating kernel metric makes KFAC model more robust against the noise. Because only global information is used,



**FIGURE 3.** Segmentation results on images with intensity inhomogeneity. First column: original images with initial contour. Second column to fifth column: segmentation results of our model, CV model, FEBAC model and LBF model, respectively.

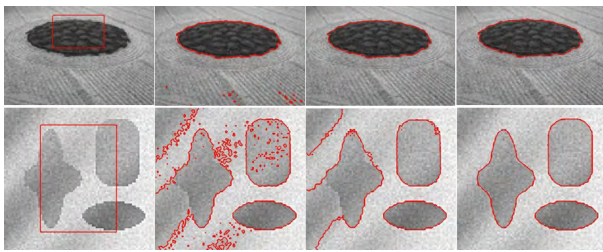


**FIGURE 4.** Comparisons with FEBAC model and KFAC model. First column: original images with initial contour. Second column to fourth column: segmentation results of FEBAC model, KFAC model and our model, respectively.

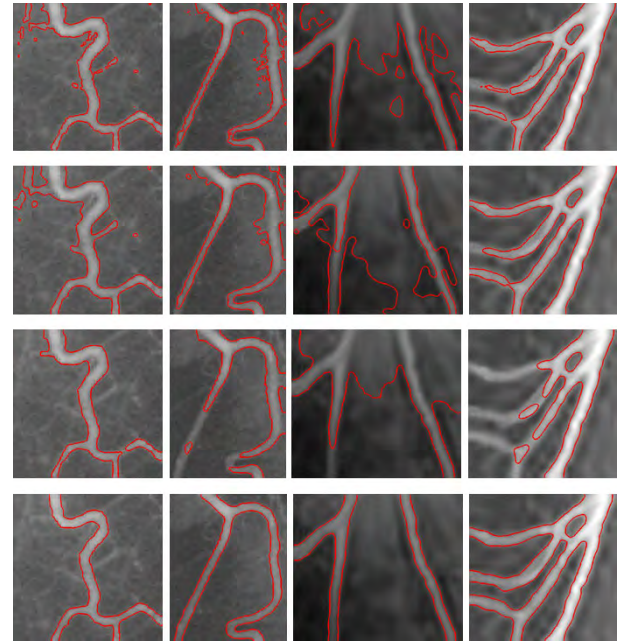
KFAC model fails to tackle intensity inhomogeneity as shown in the bottom row. In contrast, the proposed model achieves a much better performance, which benefited from the new penalty function and the usage of local fuzzy information.

**B. APPLICATION ON REAL VESSEL IMAGES**

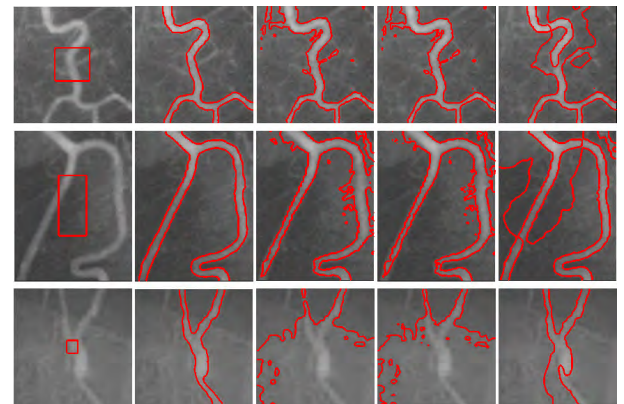
Intensity inhomogeneity often occurs in real vessel images. In this section, comparisons are made to validate the performance of our model. Figure 5 shows the comparisons with FEBAC model, SLSS model and KFAC model on real vessel images. First row to fourth row show the segmentation results of FEBAC model, SLSS model, KFAC model and our model, respectively. The segmentation results show desirable performance of the proposed model over these fuzzy logic based methods in terms of accuracy.

Figure 6 and Figure 7 show the vessel segmentation of different modalities. Figure 6 shows the segmentation results of three vessel images with intensity inhomogeneity. Two digital subtraction angiography (DSA) images and one infrared fundus vessel image with initial contours are shown in the first column. Figure 7 shows the segmentation results for different vessel images: abdominal vessel (computed tomography, CT), carotid vessel (magnetic resonance angiography, MRA), and pulmonary vessel (ultrasonic imaging, US). They are shown in the first column from top to bottom. In Figure 6 and Figure 7, the segmentation results of our model, CV model, FEBAC model, LBF model are shown from the second column to the last column, respectively.

In Figure 6, vessel images with weak boundaries render it a nontrivial problem to segment them. From the segmentation



**FIGURE 5.** Comparisons with FEBAC model, SLSS model and KFAC model. First row to fourth row: segmentation results of FEBAC model, SLSS model, KFAC model and our model, respectively.



**FIGURE 6.** Segmentation results on DSA and infrared vessel images. First column: original images with initial contour. Second column to fifth column: segmentation results of our model, CV model, FEBAC model and LBF model, respectively.

results, we can see that the compared models fail to segment these images. In contrast, our model obtains satisfactory segmentation results. The reason is that incorporating local fuzzy statistical information into the model makes our model more effective to cope with intensity inhomogeneity. In Figure 7, the segmentation results of CV model and FEBAC model are better than the LBF model, because the global based models are more robust than the local based models, which are easily trapped into local minimum. Compared with CV model and FEBAC model, the proposed model can accurately segment the weak boundaries. Compared with LBF model, our model is more robust.

Figure 8 shows the segmentation results of four retinal vessel images. These images exhibit low contrast and weak

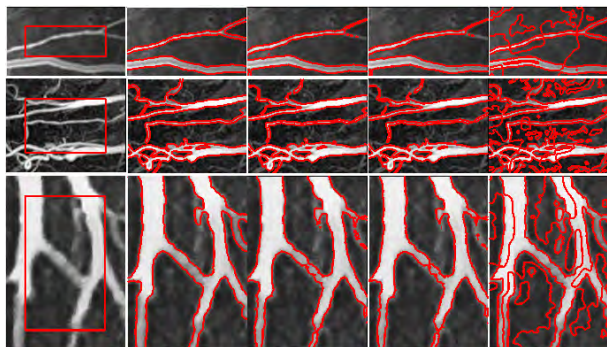


**FIGURE 7.** Segmentation results on CT, MRA and US vessel images. First column: original images with initial contour. Second column to fifth column: segmentation results of our model, CV model, FEBAC model and LBF model, respectively.

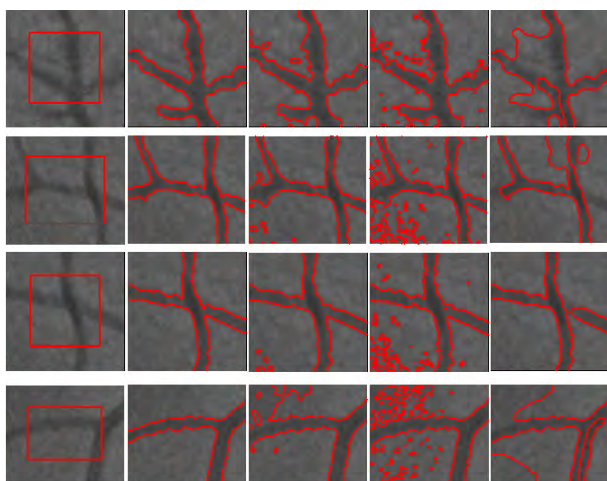


**FIGURE 8.** Segmentation results on retinal vessel images. First column: original images with initial contour. Second column to fifth column: segmentation results of our model, CV model, FEBAC model and LBF model, respectively.

boundaries and are shown in the first column from top to bottom. Each row corresponding to the original image with initial contour and the final evolution results of our model, CV model, FEBAC model and LBF model, respectively. The segmentation results demonstrate that the proposed model can extract the real vessel boundaries accurately. Because our model is not directly defined on the original image, but is defined on the enhanced image, which makes the proposed model work well on low contrast vessel images.

### C. ROBUSTNESS TO INITIAL CONTOURS

To further evaluate the capability of our model in coping with intensity inhomogeneity and its robustness to initial contours, we apply our model and LBF model to segment two vessel images with different initial contours. Figure 9 and Figure 10 show the segmentation results. The first row shows the five different initializations. The second row is the results of our model. The third row is the results of LBF model. From the segmentation results, we can see that LBF model can get

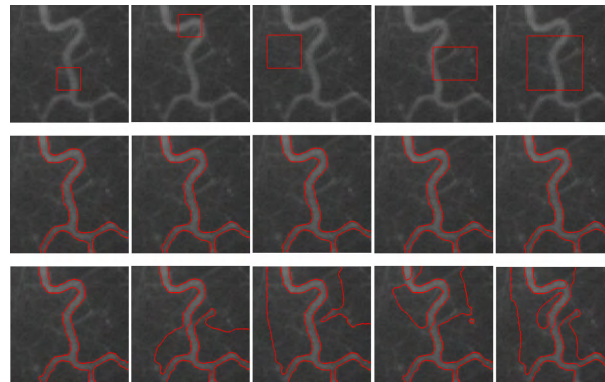


**FIGURE 9.** Segmentation results on a vessel image with different initial contours. First row: original image with initial contour. Second row: segmentation results of our model. Third row: segmentation results of LBF model.

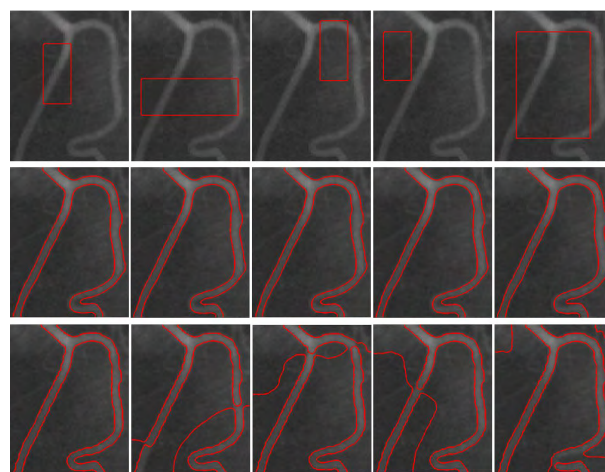


**FIGURE 10.** Segmentation results on a vessel image with different initial contours. First row: original image with initial contour. Second row: segmentation results of our model. Third row: segmentation results of LBF model.

accurate segmentation results on image with the first initial contour, but fails to segment others, because the local statistical information used by the LBF model is easily affected by the intensity of a certain point. In contrast, our model has desirable performance on images with five different initial contours. In other words, our model is less sensitive to initial contour than LBF model owe to considering not only local statistical information but also fuzzy clustering method.

### V. CONCLUSION

In this paper, we propose a robust local fuzzy active contour model for vascular segmentation. It incorporates the fuzzy local statistical information into the model by the usage of a Gaussian kernel function. Moreover, our model is not directly defined on the original image, but is defined on the image enhanced by the designed fractional-order differential operation. The proposed model overcomes the drawbacks of traditional local energy-based models, which highly depend on the position of initial contour. Meanwhile, the proposed

model works well on images with inhomogeneous intensity and low contrast. In addition, our model allows for a flexible initialization. Experimental results demonstrate the desirable performance of our model for vessel images with inhomogeneity in terms of accuracy and robustness.

## REFERENCES

- [1] J. Thangavel et al., "The vascular endothelium and human diseases," *Int. J. Biol. Sci.*, vol. 9, no. 10, pp. 1057–1069, Nov. 2013.
- [2] S. Davis, S. Mendis, and B. Norrving, "Organizational update: The World Health Organization global status report on noncommunicable diseases 2014; one more landmark step in the combat against stroke and vascular disease," *Stroke*, vol. 46, no. 5, pp. e121–e122, May 2015.
- [3] J. S. Suri, K. Liu, L. Reden, and S. Laxminarayan, "A review on MR vascular image processing: Skeleton versus nonskeleton approaches: Part II," *IEEE Trans. Inf. Technol. Biomed.*, vol. 6, no. 4, pp. 338–350, Dec. 2002.
- [4] C. Scharfenberger, A. G. Chung, A. Wong, and D. A. Clausi, "Salient region detection using self-guided statistical non-redundancy in natural images," *IEEE Access*, vol. 4, pp. 48–60, 2016.
- [5] M. Hernandez and A. F. Frangi, "Non-parametric geodesic active regions: Method and evaluation for cerebral aneurysms segmentation in 3DRA and CTA," *Med. Image Anal.*, vol. 11, no. 3, pp. 224–241, Jun. 2007.
- [6] R. Manniesing, B. K. Velthuis, M. S. van Leeuwen, I. C. van der Schaaf, P. J. van Laar, and W. J. Niessen, "Level set based cerebral vasculature segmentation and diameter quantification in CT angiography," *Med. Image Anal.*, vol. 10, no. 2, pp. 200–214, Apr. 2006.
- [7] M. S. Hassouna, A. A. Farag, S. Hushek, and T. Moriarty, "Cerebrovascular segmentation from TOF using stochastic models," *Med. Image Anal.*, vol. 10, no. 1, pp. 2–18, Feb. 2006.
- [8] R. Gan, W. C. Wong, and A. C. Chung, "Statistical cerebrovascular segmentation in three-dimensional rotational angiography based on maximum intensity projections," *Med. Phys.*, vol. 32, no. 9, pp. 3017–3028, Sep. 2005.
- [9] S. Worz and K. Rohr, "Segmentation and quantification of human vessels using a 3-D cylindrical intensity model," *IEEE Trans. Image Process.*, vol. 16, no. 8, pp. 1994–2004, Aug. 2007.
- [10] W. C. K. Wong and A. C. S. Chung, "Bayesian image segmentation using local iso-intensity structural orientation," *IEEE Trans. Image Process.*, vol. 14, no. 10, pp. 1512–1523, Oct. 2005.
- [11] G. Yu, Y. L. Miao, P. Li, and Z. Z. Bian, "Multiscale active contour model for vessel segmentation," *J. Med. Eng. Technol.*, vol. 32, no. 1, pp. 1–9, Jan./Feb. 2008.
- [12] Y. Shang et al., "Vascular active contour for vessel tree segmentation," *IEEE Trans. Biomed. Eng.*, vol. 58, no. 4, pp. 1023–1032, Apr. 2011.
- [13] Z. Wang, X. Wei, W. Huang, J. Zhou, and S. K. Venkatesh, "A fuzzy clustering vessel segmentation method incorporating line-direction information," *Proc. SPIE*, vol. 8314, p. 83143I, Feb. 2012.
- [14] J. Z. Yang, S. Ma, W. J. Tan, Q. Sun, P. Cao, and D. Z. Zhao, "MRA fuzzy c-means vessel segmentation algorithm based on tubular structure," *J. Med. Imag. Health Inform.*, vol. 5, no. 8, pp. 1853–1858, Dec. 2015.
- [15] J. C. Bezdek, *Pattern Recognition With Fuzzy Objective Function Algorithms*. New York, NY, USA: Plenum, 1981.
- [16] V. Estellers, D. Zosso, R. Lai, S. Osher, J. P. Thiran, and X. Bresson, "Efficient algorithm for level set method preserving distance function," *IEEE Trans. Image Process.*, vol. 21, no. 12, pp. 4722–4734, Dec. 2012.
- [17] V. Caselles, F. Catté, T. Coll, and F. Dibos, "A geometric model for active contours in image processing," *Numer. Math.*, vol. 66, no. 1, pp. 1–31, Dec. 1993.
- [18] V. Caselles, R. Kimmel, and G. Sapiro, "Geodesic active contours," *Int. J. Comput. Vis.*, vol. 22, no. 1, pp. 61–79, Feb. 1997.
- [19] T. F. Chan and L. A. Vese, "Active contours without edges," *IEEE Trans. Image Process.*, vol. 10, no. 2, pp. 266–277, Feb. 2001.
- [20] C. Li, C.-Y. Kao, J. C. Gore, and Z. Ding, "Implicit active contours driven by local binary fitting energy," in *Proc. IEEE Conf. Comput. Vis. Pattern Recognit.*, Jun. 2007, pp. 1–7.
- [21] C. Li, C.-Y. Kao, J. C. Gore, and Z. Ding, "Minimization of region-scalable fitting energy for image segmentation," *IEEE Trans. Image Process.*, vol. 17, no. 10, pp. 1940–1949, Oct. 2008.
- [22] D. Mumford and J. Shah, "Optimal approximations by piecewise smooth functions and associated variational problems," *Commun. Pure Appl. Math.*, vol. 42, no. 5, pp. 577–685, 1989.
- [23] K. Zhang, H. Song, and L. Zhang, "Active contours driven by local image fitting energy," *Pattern Recognit.*, vol. 43, no. 4, pp. 1199–1206, Apr. 2010.
- [24] S. Krinidis and V. Chatzis, "Fuzzy energy-based active contours," *IEEE Trans. Image Process.*, vol. 18, no. 12, pp. 2747–2755, Dec. 2009.
- [25] T.-T. Tran, K.-K. Shyu, V.-T. Pham, and P.-L. Lee, "Global and local fuzzy energy-based active contours for image segmentation," *Nonlinear Dyn.*, vol. 67, no. 2, pp. 1559–1578, Jan. 2012.
- [26] Q. T. Thieu, M. Luong, J.-M. Rocchisani, N. Linh-Trung, and E. Viennet, "Novel active contour model for image segmentation based on local fuzzy Gaussian distribution fitting," *J. Electron. Sci. Technol.*, vol. 10, no. 2, pp. 113–118, Jun. 2012.
- [27] Y. Wu, W. Ma, M. Gong, H. Li, and L. Jiao, "Novel fuzzy active contour model with kernel metric for image segmentation," *Appl. Soft. Comput.*, vol. 34, pp. 301–311, Sep. 2015.
- [28] B. N. Li, J. Qin, R. Wang, M. Wang, and X. Li, "Selective level set segmentation using fuzzy region competition," *IEEE Access*, vol. 4, pp. 4777–4788, 2016.
- [29] S. Fu, Q. Ruan, W. Wang, F. Gao, and H.-D. Cheng, "A feature-dependent fuzzy bidirectional flow for adaptive image sharpening," *Neurocomputing*, vol. 70, no. 4, pp. 883–895, Jan. 2007.
- [30] S. J. Fu, C. Zhang, and X. Tai, "Image denoising and deblurring: Non-convex regularization, inverse diffusion and shock filter," *Sci. China Inf. Sci.*, vol. 54, no. 6, pp. 1184–1198, Jun. 2011.
- [31] Y.-F. Pu, J.-L. Zhou, and X. Yuan, "Fractional differential mask: A fractional differential-based approach for multiscale texture enhancement," *IEEE Trans. Image Process.*, vol. 19, no. 2, pp. 491–511, Feb. 2010.
- [32] S. Khanna and V. Chandrasekaran, "Fractional derivative filter for image contrast enhancement with order prediction," in *Proc. IET Conf. Image Process. (IPR)*, 2012, pp. 1–6.
- [33] N. He, J.-B. Wang, L.-L. Zhang, and K. Lu, "An improved fractional-order differentiation model for image denoising," *Signal Process.*, vol. 112, pp. 180–188, Jul. 2015.
- [34] B. Li and W. Xie, "Adaptive fractional differential approach and its application to medical image enhancement," *Comput. Elect. Eng.*, vol. 45, pp. 324–335, Jul. 2015.
- [35] B. Li and W. Xie, "Image denoising and enhancement based on adaptive fractional calculus of small probability strategy," *Neurocomputing*, vol. 175, pp. 704–714, Jan. 2016.
- [36] M. Sussman, P. Smereka, and S. Osher, "A level set approach for computing solutions to incompressible two-phase flow," *J. Comput. Phys.*, vol. 114, no. 1, pp. 146–159, Sep. 1994.

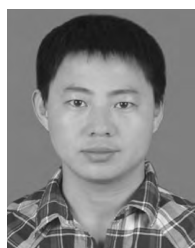


image segmentation.

**HONGLI LV** received the B.S. degree from the School of Mathematics and Statistics, Henan University, Kaifeng, China, in 2007, and the M.S. degree from the College of Mathematics and Information Science from Wenzhou University, Wenzhou, China, in 2015. He is currently pursuing the Ph.D. degree with the School of Mathematics, Shandong University, China. His research interests include medical image processing and computer vision, especially image denoising and



**ZIYU WANG** received the B.S. degree in radiology from Shandong Medical College in 1999. He is currently a Physician with the Department of Radiology, Yidu Central Hospital of Weifang, China. He has authored several papers in important medical journals and conferences. His research interests include medical imaging and medical image quality assessment.





**SHUJUN FU** received the B.S. degree in power engineering and the M.S. degree in computational mathematics from Shandong University in 1990 and 1999, respectively, and the Ph.D. degree in signal and information processing from Beijing Jiaotong University in 2009. He is currently a Professor with the School of Mathematics, Shandong University. He has authored about 60 papers in important journals and conferences. His research interests include image

processing, partial differential equations, numerical computing, medical imaging, image measurement, and target detection and recognition. He is also a Peer Reviewer on some important journals.



**LIN ZHAI** received the B.S. degree from the School of Information Science and Engineering from Dalian Ocean University, Dalian, China, in 2011, and the M.S. degree from the School of Computer and Information Engineering from Inner Mongolia Agricultural University, Hohhot, China, in 2014. She is currently pursuing the Ph.D. degree with the School of Mathematics, Shandong University, Jinan, China. Her research interests include medical image denoising and

pattern recognition.



**CAIMING ZHANG** received the B.S. degree and the M.E. degree in computer science from Shandong University in 1982 and 1984, respectively, and the Dr.Eng. degree in computer science from the Tokyo Institute of Technology, Japan, in 1994. He is currently a Professor and the Doctoral Supervisor with the School of Computer Science and Technology, Shandong University. From 1997 to 2000, he has held visiting position with the University of Kentucky, USA.

His research interests include CAGD, CG, information visualization, and medical image processing.



**XUYA LIU** received the B.S. degree from the School of Mathematics, Qufu Normal University, China, in 2014. She is currently pursuing the Ph.D. degree with the School of Mathematics, Shandong University, China. She has been taking successive postgraduate and doctoral programs of study for doctoral degree, since 2014. Her research interests are medical image processing and image analysis, especially in image denoising.

...